

PAPER

Electrostatic interaction of heterogeneously charged surfaces with semipermeable membranes

Salim R. Maduar,^{ab} Vladimir Lobaskin^c and Olga I. Vinogradova^{*abd}

Received 28th June 2013, Accepted 17th July 2013

DOI: 10.1039/c3fd00101f

In this paper we study the electrostatic interaction of a heterogeneously charged wall with a neutral semipermeable membrane. The wall consists of periodic stripes, where the charge density varies in one direction. The membrane is in contact with a bulk reservoir of an electrolyte solution and separated from the wall by a thin film of salt-free liquid. One type of ions (small counterions) permeates into the gap. This gives rise to a distance-dependent membrane potential, which translates into a repulsive electrostatic disjoining pressure due to an overlap of counterion clouds in the gap. To quantify it we use two complementary approaches. First, we propose a mean-field theory based on a linearized Poisson–Boltzmann equation and Fourier analysis. These calculations allow us to estimate the effect of a heterogeneous charge pattern at the wall on the induced heterogeneous membrane potential, and the value of the disjoining pressure as a function of the gap. Second, we perform Langevin dynamics simulations of the same system with explicit ions. The results of the two approaches are in good agreement with each other at low surface charges and small gaps, but differ due to nonlinearity at higher charges. These results demonstrate that a heterogeneity of the wall charge can lead to a huge reduction in the electrostatic repulsion, which could dramatically facilitate self-assembly in complex synthetic and biological systems.

1 Introduction

Long-range electrostatic interactions between surfaces play a central role in a variety of biological processes and substantially influence the properties of colloidal suspensions, thin films, and nanostructured materials. Most theoretical and experimental studies of electrostatic forces have been conducted for

^aA. N. Frumkin Institute of Physical Chemistry and Electrochemistry, Russian Academy of Sciences, 31 Leninsky Prospect, 119991 Moscow, Russia

^bFaculty of Physics, M. V. Lomonosov Moscow State University, 119991 Moscow, Russia

^cSchool of Physics and Complex and Adaptive Systems Laboratory, University College Dublin, Belfield, Dublin 4, Ireland

^dDWI, RWTH Aachen, Forckenbeckstr. 50, 52056 Aachen, Germany

symmetric systems, and by assuming that the surfaces are homogeneously charged and impermeable.¹ In this paper we focus on an asymmetric case of interactions of a patterned impermeable wall with a neutral semi-permeable membrane, as a boundary to an aqueous electrolyte solution.

Surfaces with inhomogeneous charge distributions are of importance for several reasons. First, such inhomogeneous systems are ubiquitous, especially in biology. The best-known examples are the proteins, cellular membrane lipids,² soft anisotropic materials,³ and self-assembled molecular layers on charged surfaces.^{4–6} Second, the methods of surface treatment have advanced considerably during the past decade and enabled the fabrication of charge patterns in systems such as spherical Janus particles⁷ and various patchy objects.^{8,9} Third, they model the effect of defects in homogeneous systems. In an effort to better understand the connection between the heterogeneity of a charge distribution and the amplitude of repulsive forces, the interaction of patterned walls in a liquid has been studied by several groups. Experimental studies have been performed to quantify the interaction between charged^{4–6} and neutral surfaces, where the average charge is zero,^{10,11} with different distributions of surface charge heterogeneities. Most theoretical effort has been focussed on the interaction between two periodically patterned surfaces^{12–14} using the linearized Poisson–Boltzmann (PB) equation, and boundary conditions of a fixed surface charge density (or a fixed surface potential) for the heterogeneous patterns. These studies concluded that for heterogeneously charged surfaces with a non-zero total charge the leading-order interaction is dominated by the average charge, and that the repulsion between the surfaces becomes weaker than between two uniformly charged surfaces with the same average charge. However, for overall neutral surfaces the interaction of charge patches depends on the location and periodicity of the pattern and can change from being repulsive to attractive. Another recent development includes investigations of systems with randomly distributed charges,¹⁵ strong correlations in systems with mobile charges,^{16,17} charge regulation, and non-linear ionic screening in heterogeneous systems.¹⁸

Donnan equilibria, which arise in the presence of semipermeable membranes, are of considerable importance in many areas of science and technology. Well known examples of semipermeable membranes are synthetic liposomes with ion channels,¹⁹ and multilayer shells of polyelectrolyte microcapsules.^{20–23} Biological examples include viral capsids,²⁴ cell²⁵ and bacterial^{26–28} membranes. Since they were discovered, the theory of Donnan equilibria mainly focussed on the case of a single membrane,^{29,30} or a single vesicle/capsule.^{29,31–34} However, ion equilibria play a very important role in processes determining various interactions with membranes. The quantitative understanding of electrostatic interactions involving membranes is still challenging. Previous investigations were restricted to interactions of two model membranes and relied on a number of assumptions and simplifications. Some solutions of the PB equation are known for charge bearing ionizable groups immersed in salt reservoirs.³⁵ Later works in this direction assumed that the membranes are uncharged, and are separated by a thin film of salt-free solvent.³⁶ Results were not limited by calculations within the PB theory, and also included Langevin dynamics simulations with explicit ions. In the wide gap limit, a repulsive disjoining pressure was predicted. Recent integral equation studies suggested charge correlation effects in large concentration solutions of multivalent ions that could result in short-range attractions.³⁷ We are

unaware of any previous work that has addressed the question of the interaction of a semipermeable membrane with a wall.

In this paper, we explore the charge and potential distributions arising when a neutral semipermeable membrane as a boundary to the electrolyte solution, is separated by a thin film of background solvent from the charged wall decorated by stripes with fixed densities of a local surface charge. We first solve analytically a linearized PB equation for a weak local charge, and evaluate the distribution of electrostatic potential in the system. We then derive an explicit expression for the pressure on the membranes and a disjoining pressure in the gap between them. Our mean-field approach is verified by Langevin dynamics simulations.

2 Theory

We consider a system consisting of a charged impermeable wall and a semi-permeable membrane in contact with an electrolyte solution. The gap between the wall and the membrane, h , is filled with a salt-free solvent (Fig. 1). We assume that the membrane is permeable to one type of ion (small ions or counter-ions) with charge ze and impermeable to another type (large ions) with charge $|Ze| \geq |ze|$. Here, Z and z are the valencies of the large and small ions, respectively, and e is the elementary charge. The ion concentrations are denoted by C for large ions and c for small ions. The membrane is infinitesimally thin, rigid, and electrically neutral. We focus on a periodic, charged, striped wall with an average charge density σ^s , where the charge and the potential, ψ , are varying in only one direction, y , with a periodicity L . Alternating stripes are characterized by charge densities σ_1^s and σ_2^s . The surface fraction of stripes of type 1 is denoted as $\omega = L_1/L$, where L_1 is the width of the stripe with charge density σ_1^s . The permittivities of the inner and outer solutions are equal and denoted below as ϵ .

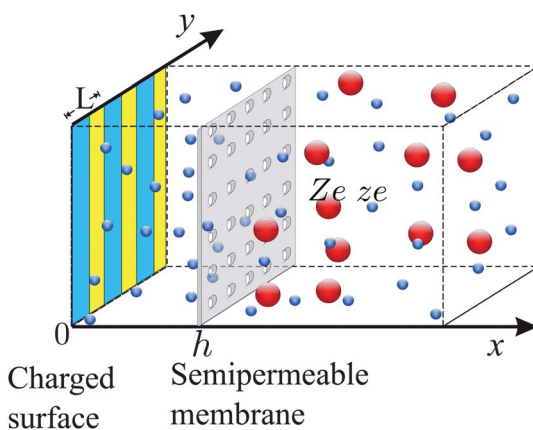


Fig. 1 Schematic of the studied system consisting of a neutral semipermeable membrane at $x = h$ with a heterogeneously charged surface at $x = 0$. The period of the charge distribution is denoted by L . Small spheres indicate small ions. The large ions are also depicted as spherical, which is appropriate, for instance, for conventional charged colloids, nanogels or micelles, but our conclusions are general. They could also apply for cylindrical species, e.g., DNA, viruses, actin filaments or polyelectrolytes.

2.1 Potential

We first introduce the dimensionless electrostatic potentials $\varphi_{i,o} = \frac{ze\psi_{i,o}}{k_B T} \ll 1$ with the indices i and o standing for “in” ($x < h$) and “out” ($x \geq h$) of the confined slab.³⁶ We then assume a weakly charged surface, so that φ satisfies the linearized PB equations:

$$\Delta\varphi_i(x, y) = \kappa_i^2(\varphi_i(x, y) - 1), \quad 0 < x < h \quad (1)$$

$$\Delta\varphi_o(x, y) = \kappa_o^2\varphi_o(x, y), \quad x \geq h, \quad (2)$$

where the inner inverse screening length, κ_i^{-1} , is defined as $\kappa_i^2 = 4\pi\ell_B c_0$ with $\ell_B = z^2 e^2 / (4\pi\epsilon k_B T)$ the Bjerrum length, $\tilde{Z} = Z/z < 0$ is the valence ratio of large and small ions, and c_0 is the bulk concentration of small ions in the outer space. The outer inverse screening length, κ_o , can be calculated as $\kappa_o^2 = 4\pi\ell_B(\tilde{Z}^2 C_0 + c_0)$, where C_0 is the concentration of large ions far from the membrane. Obviously, this represents the inverse Debye length of the bulk electrolyte solution in the container. Enforcing the electroneutrality $ZC_0 + zc_0 = 0$, we find $\kappa_o = \kappa_i\eta$, where $\eta = \sqrt{1 - \tilde{Z}}$. Note that for this particular problem, the main reference length scale that determines the behavior of the system is κ_i^{-1} , as we show below.

We solve these equations with a boundary condition of prescribed surface charge $\sigma^s(y)$ on the wall and continuity of the electric field at $x = h$ which corresponds to the case of a neutral membrane:

$$\partial_x \varphi_i(x, y)|_{x=0} = -\frac{4\pi ze}{\epsilon k_B T} \sigma^s(y) = -b(y), \quad (3)$$

$$\partial_x \varphi_i(x, y)|_{x=h} = \partial_x \varphi_o(x, y)|_{x=h}, \quad (4)$$

where $b(y) = \frac{4\pi ze}{\epsilon k_B T} \sigma^s(y)$ is a local analogue of the Gouy–Chapman inverse length. In our case of alternating stripes $b(y)$ switches between two values, b_1 and b_2 . Parameter $b_{1,2}\kappa_i^{-1}$ then characterizes the interplay between ion–ion and ion–wall interactions.³⁸

Note that at high charge densities and high values of the electric potential, the description of the problem cannot be simplified by linearization of the PB approach. Beside that, correlations between macroions should be taken into account in the limit of large charges Z . Based on earlier results,³³ one can expect to observe the same qualitative picture at least at low polyion concentrations, while at the higher concentrations the correlation effects might become significant.³⁷ We leave the study of the latter regime for a future work.

Applying boundary conditions (4) to eqn (1) and (2) we obtain a distribution of the potential:

$$\begin{aligned} \varphi_i(x, y) = 1 + & \frac{b_0\kappa_i^{-1}\cosh[\kappa_i(h-x)] - \eta_0\cosh[\kappa_i x] + \eta_0 b_0\kappa_i^{-1}\sinh[\kappa_i(h-x)]}{\eta_0\cosh[\kappa_i h] + \sinh[\kappa_i h]} \\ & + \sum_{n \neq 0} \frac{b_n \cosh[q_n(h-x)] + \eta_n \sinh[q_n(h-x)]}{\eta_n \cosh[q_n h] + \sinh[q_n h]} e^{ik_n y}, \end{aligned} \quad (5)$$

where b_n is the Fourier coefficient of $b(y)$, $k_n = \frac{2\pi n}{L}$, $q_n^2 = k_n^2 + \kappa_i^2$, and $\eta_n^2 = \frac{k_n^2 + \kappa_o^2}{q_n^2}$. The average dimensionless surface charge is $b_0\kappa_i^{-1}$, where $b_0 = b_1\omega + b_2(1 - \omega)$.

2.2 Disjoining pressure

At the equilibrium, the disjoining pressure consists of two parts, namely, the pressure due to the electric volume force ($\rho\mathbf{E}$) and the ideal osmotic pressure.³⁹ Within the linearized PB theory, one should replace the boundary density rule from the nonlinear PB theory by its linear case analogue.^{33,40} Below we discuss this for our system.

A mechanical equilibrium requires that the solution for the potential and charge distribution satisfy the hydrostatic equation

$$0 = -\nabla p + \rho\mathbf{E} = \nabla \cdot (\mathbb{T} - \mathbb{I}p) \equiv -\nabla \cdot \Pi \quad (6)$$

where \mathbb{T} is Maxwell's electrostatic stress tensor

$$\mathbb{T}_{ij} = \frac{\varepsilon}{4\pi} \left[E_i E_j - \delta_{ij} \frac{\mathbf{E}^2}{2} \right] \quad (7)$$

The difference, $\Pi(x, y) = \mathbb{T}(x, y) - \mathbb{I}p(x, y)$, represents an electrostatic disjoining pressure, which is equal to the excess osmotic pressure at the particular position in the film, x_0 , where the magnitude of potential has a minimum value, and the electrostatic stress vanishes ($\mathbb{T} = 0$).^{36,38,41,42} The interaction force for heterogeneous objects is a surface integral of $\Pi \cdot \bar{\mathbf{n}}_s$.⁴³⁻⁴⁵ Therefore, to find x_0 for our system, which now could depend on y , we propose to use a y -average disjoining pressure $\frac{1}{L} \int_{y=0}^{y=L} \Pi(x, y) \equiv \langle \Pi(x, y) \rangle_y dy$, as a measure of an electrostatic interaction. We then use eqn (6) to calculate the average disjoining pressure

$$\langle \Pi(x_0, y) \rangle_y = \langle p - \mathbb{T} \rangle_y = \langle p(x_0, y) \rangle_y \approx k_B T c_0 (1 - \langle \varphi_i(x_0, y) \rangle_y) \quad (8)$$

To calculate the value of a potential at the (still unknown) point, x_0, y_0 , we have to find a relationship between the field and the potential. This can be done by multiplying eqn (1) by $\nabla\varphi \equiv \{\partial_x\varphi, \partial_y\varphi\}$. Taking into account that $\mathbf{E} = -\nabla\varphi \frac{k_B T}{ze}$, we find:

$$-\nabla \left[\frac{\mathbb{T}}{k_B T c_0} - \left(\frac{\varphi_i^2(x, y)}{2} - \varphi_i(x, y) \right) \mathbb{I} \right] = 0 \quad (9)$$

The off-diagonal components represent the *tangential force* on the charged surface, which should vanish on average. The y -averaging of eqn (9) then eliminates these components of the Maxwell stress tensor $\langle \mathbb{T}_{xy} \rangle = \langle \mathbb{T}_{yx} \rangle = 0$:

$$\frac{\partial}{\partial x} \left\langle \frac{(\partial_x \varphi_i)^2 - (\partial_y \varphi_i)^2}{2\kappa_i^2} + \left(\frac{\varphi_i^2(x, y)}{2} - \varphi_i(x, y) \right) \right\rangle_y = 0 \equiv \frac{\partial}{\partial x} C(h) \quad (10)$$

where $C(h)$ is an integration constant for the linearized PB equation. Comparing eqn (9) and (10) to eqn (6), we derive

$$p(x, y) = A + k_{\text{B}} T c_0 \left(\frac{\varphi_i^2(x, y)}{2} - \varphi_i(x, y) \right) \quad (11)$$

Following this approach^{33,36,40} we find the constant A by using van't Hoff's law at the position of the minimum-magnitude potential, x_0 :

$$p(x, y) = k_{\text{B}} T c(x_0, y) + k_{\text{B}} T c_0 \left(\frac{\varphi_i^2(x, y) - \varphi_i^2(x_0, y)}{2} - (\varphi_i(x, y) - \varphi_i(x_0, y)) \right) \quad (12)$$

After solving the linearized PB equation for φ , one can verify that the left-hand side of eqn (10), *i.e.* $C(h)$, does not depend on x but can be a function of separation, h . Without loss of generality, we then can calculate the constant by using eqn (10) at $x = h$:

$$C(h) = \left\langle \frac{\tilde{Z}}{2} \varphi^m(y)^2 - \varphi^m(y) \right\rangle_{y\text{-average}}, \quad (13)$$

where φ^m is the potential of a membrane.

Now we set $E_x = E_y = 0$ in eqn (10) and solve it with respect to $\varphi(x_0) \equiv \varphi|_{\mathbb{T}(x_0, y)} = 0$:

$$\left\langle \frac{1}{2} \varphi^2(x_0, y) - \varphi(x_0, y) \right\rangle_y = C(h) \quad (14)$$

By substituting this into eqn (8), we obtain an expression for the disjoining pressure in the gap between the semipermeable membrane and the heterogeneously charged surface:

$$\left(\frac{\Pi(h)}{k_{\text{B}} T c_0} \right)^2 = 1 + 2C(h) = 1 + \left\langle \tilde{Z} \varphi^m(y)^2 - 2\varphi^m(y) \right\rangle_{y\text{-average}} \quad (15)$$

A remarkable corollary of this relationship is that the disjoining pressure can be easily determined once the induced membrane potential is found.

3 Simulation

The Langevin dynamics (MD) simulations are performed on the level of the primitive model with explicit large and small ions using the ESPResSo simulation package.⁴⁶ Our model also includes a charged surface and neutral semipermeable membrane. The membranes are made impermeable for cations, but "invisible" for anions.³²

All electrolyte ions repel each other with a repulsive Weeks–Chandler–Andersen (WCA) potential⁴⁷ of range σ_{WCA} and magnitude ε_{WCA} . The same potential acts between the particles and the walls (charged surfaces and semipermeable membranes). To illustrate our approach, we here use only a monovalent electrolyte ($Z = 1$, $z = -1$). The temperature is set by a Langevin thermostat to $k_{\text{B}} T = 1.0 \varepsilon_{\text{WCA}}$.

The solvent is treated as a homogeneous medium with a dielectric permittivity set through the Bjerrum length ℓ_{B} . The electrostatic interaction between the ionic

species is modelled by the Coulomb potential $U_{\text{Coul}}(r_{ij}) = k_{\text{B}}T \frac{\ell_{\text{B}} q_i q_j}{r_{ij}}$, where $q_i = \pm 1$ with $\ell_{\text{B}} = 0.8\sigma_{\text{WCA}}$ to $1\sigma_{\text{WCA}}$. We model the systems with 2D-periodicity in the y and z directions to exclude any boundary effects. The electrostatic interactions are calculated using the P3M⁴⁸ method combined with the electrostatic layer correction (ELC)-algorithm⁴⁹ with gap size $50\sigma_{\text{WCA}}$.

Bulk ion concentrations vary from $10^{-4}\sigma_{\text{WCA}}^{-3}$ to $10^{-3}\sigma_{\text{WCA}}^{-3}$, which gives the screening length in the range $\kappa_i^{-1} = 6\sigma_{\text{WCA}}$ to $20\sigma_{\text{WCA}}$. We verified that the force exerted on the surface depends on the dimensionless parameter $\kappa_i h$ rather than on κ_i or h separately. Therefore for force measurements for κh we fixed $\kappa_i^{-1} = 10\sigma_{\text{WCA}}$ and varied h in the range from $3\sigma_{\text{WCA}}$ to $70\sigma_{\text{WCA}}$. These values allow us to calculate the interaction force for a wide range of dimensionless separations $\kappa_i h = 0.3$ – 20 .

A *charged plate* is constructed from discrete charges at surface density $\sigma^s = 10^{-2}q_{\text{s}}e \times \sigma_{\text{WCA}}^{-2}$, where $q_{\text{s}}e$ is the charge of a discrete surface ion. The surface charges are located at $x = 0$ and random $\{y, z\}$ coordinates. In our system, the inverse Gouy–Chapman length is equal to $b = 0.1\sigma$ so that $b\kappa^{-1} = 1$. To model heterogeneity we used a periodic charge pattern with stripe widths $L_1 = L_2 = 50\sigma$. This gives the fraction of the charged stripe $\omega = 0.5$ at which heterogeneity effects are the most pronounced. Dimensionless periodicity could be varied in a wide range up to $\kappa_i L \approx 10$.

We use a *simulation box* of depth $L_x = 100\sigma_{\text{WCA}}$ – $200\sigma_{\text{WCA}}$ in the x direction, which is confined by impermeable walls at both ends ($x = 0$ and $x = L_x$). The lateral dimensions $L_y \times L_z = 200\sigma_{\text{WCA}} \times 100\sigma_{\text{WCA}}$ and the number of ions ($N = 1000$ – 4500) are selected to be large enough to achieve constant bulk ion concentrations at large x , far from the membrane. The width of the simulation box in the y -direction is set so that we have at least two periods of the charge pattern within the unit cell.

We evaluated the pressure on a plate by summation of contributions of all ions. For example, the Lennard–Jones interaction force exerted by an ion on the surface located at $x = h$ is equal to:

$$F(x) = 4\epsilon_{\text{WCA}} \left(\frac{12\sigma_{\text{WCA}}^{12}}{(x-h)^{13}} - \frac{6\sigma_{\text{WCA}}^6}{(x-h)^7} \right) \quad (16)$$

The surface-averaged pressure is then

$$p = \int_{h/2}^{h+2^{1/6}\sigma} dx \langle C(x, y) \rangle_y F(x). \quad (17)$$

We measured both bulk osmotic pressure (the pressure at the end of the box $x = L_x$) and the force on the membrane exerted by large ions. The calculated bulk osmotic pressure is further used to derive the bulk concentrations c_0 and C_0 , and to normalize the disjoining pressure by the factor $k_{\text{B}}Tc_0$.

4 Results and discussion

In this section we present some example calculations based on the analytical linearized PB theory and results of Langevin dynamics simulations.

4.1 Homogeneously charged wall

We begin by studying the case of a homogeneously charged wall, which will be a reference system for our problem. Let us first focus on ion distributions in the system, which are shown in Fig. 2 *versus* x/h (symbols). Also included are the theoretical curves (dashed curves). The agreement is excellent at small $\kappa_i h$ (strong overlap of an inner double layer). Such a situation would be realistic for dilute solutions and/or a thin gap. At large $\kappa_i h$ (weak overlap of the inner ionic layers), *i.e.* thicker films and/or more concentrated solutions, a linearized PB theory fails to describe quantitatively the simulation data in the gap. In this case, the large ions are concentrated near the membrane, which is reflected by a very sharp concentration change. The values of this peak calculated within the linearized approach differ from the simulation value. Nevertheless, the linear theory is in a good qualitative agreement with the simulation data, and could safely be used as a first approximation. We would like to stress that this is neither adsorption driven by an attraction of ions to the membrane nor condensation driven by an attraction between ions. In our case, we deal with another effect, where electrostatic self-assembly of large ions and a neutral membrane is caused by attraction of large ions to inner counterions. This, in turn, is the consequence of a counterion leakage leading to an excess charge of the inner and outer regions. At large $\kappa_i h$ the concentration profiles of the small ions have a minimum, which can be used to calculate the disjoining pressure. In the case of simulation results we can employ a boundary density rule:

$$\Pi_0 = k_B T c_{\min} = k_B T c_0 + k_B T C_0 - k_B T C^m \quad (18)$$

Here and below the subscript 0 for Π corresponds to the case of a homogeneous wall. The simulation data presented in Fig. 2 are indeed in excellent

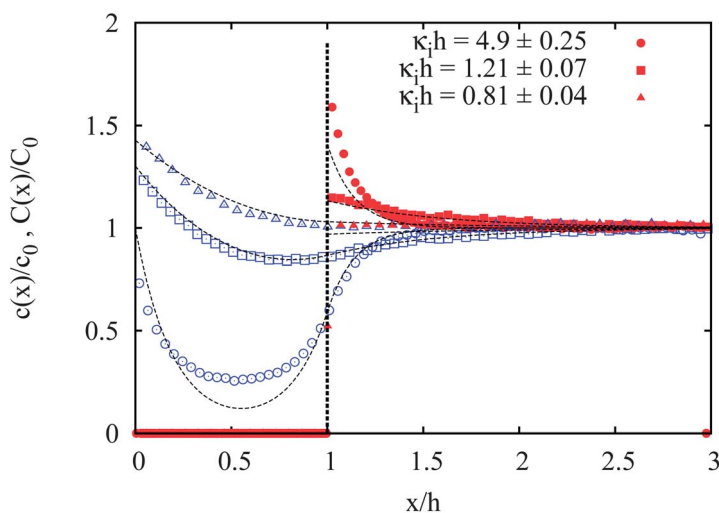


Fig. 2 Distribution of small and large ions in the system. Dashed curves show predictions of the linearized PB theory. Symbols show simulation results. Open symbols indicate small ions, filled symbols correspond to large ions.

agreement with this formula, but the linearized PB theory obviously deviates from the prediction (see ref. 33 and 40 for a detailed discussion of calculations of pressure in the linearized PB theory).

Fig. 3 shows simulation data for the disjoining pressure as a function of $\kappa_i h$ obtained for walls with different surface charges. Also included are theoretical results calculated using eqn (15). The agreement between the theory and simulations is quite good, but one can see that at large $\kappa_i h$ the linear theory underestimates the value of the disjoining pressure. The data presented in Fig. 3 show larger Π_0 at larger values of the surface charge $b_0 \kappa_i^{-1}$. Note that in the case of the uncharged wall, $b_0 = 0$, our system is equivalent to a symmetric system of two semipermeable membranes³⁶ separated by a distance two times larger, $2h$.

Finally, we note that simple asymptotic expressions can be constructed for large and small $\kappa_i h$. Thus, at the limit of large $\kappa_i h$ we derive

$$\left(\frac{\Pi_0(h)}{\kappa_B T c_0}\right)^2 \approx 4 \frac{\eta^2}{(1+\eta)^2} e^{-2\kappa_i h} - 4 \frac{b_0}{\kappa_i} \frac{\eta}{1+\eta} e^{-\kappa_i h} \quad (19)$$

These asymptotic curves are included in Fig. 3. Eqn (19) indicates qualitatively the different behavior of $\Pi_0(h)$ in the cases of neutral and charged walls. For a neutral wall the second term vanishes, and only the first term determines the decay of $\Pi_0(h)$. For charged walls the first term can safely be ignored, and the asymptotic curve is determined by the second term. In the limit of small $\kappa_i h$ we obtain

$$\left(\frac{\Pi_0(h)}{\kappa_B T c_0}\right)^2 \approx 1 - \frac{2\kappa_i b_0 \eta - b_0^2 \tilde{Z}}{\kappa_i^2 \eta^2}, \quad (20)$$

which gives the maximum value of the disjoining pressure in our system.

4.2 Heterogeneously charged wall

We begin by studying the membrane potential. Fig. 4 plots results evaluated from simulated concentration profiles [as $\varphi^m = -\log(c/c_0)$] collected in the interval of

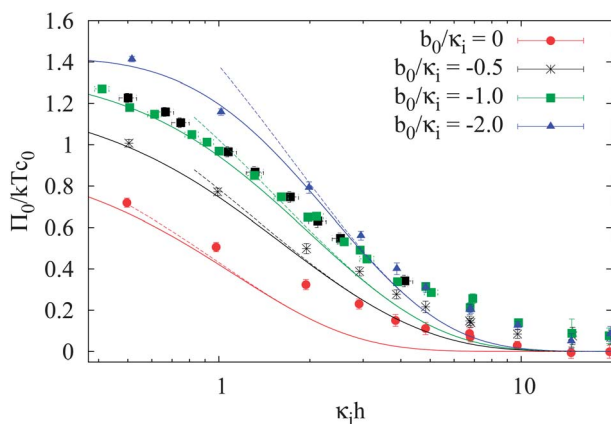


Fig. 3 Disjoining pressure in the gap between a homogeneously charged wall and a semipermeable membrane simulated at different surface charge densities on the wall (symbols). For a charge density of $b_0 \kappa_i^{-1} = -1$ data were obtained at several c_0 values. Solid curves show the predictions of the linearized PB theory [eqn (15)]. Dashed curves are asymptotic results calculated with eqn (19).

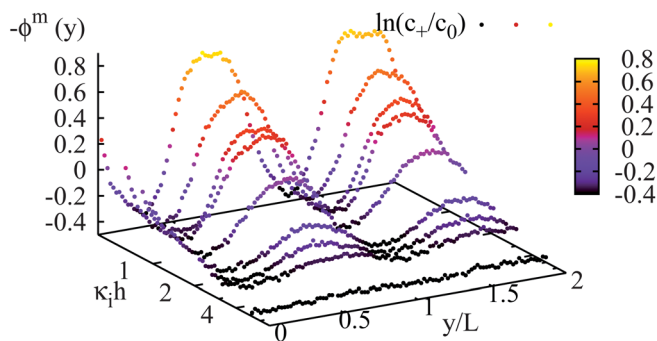


Fig. 4 Membrane potential calculated from concentration profiles collected from $x = h$ to $x = h + 2.5\sigma$. The charge density of the surface stripes is given by $b_{1,2}\kappa_i^{-1} = -1 \pm 2$.

Δx from h to $h + 0.25\kappa_i^{-1}$. The simulation data demonstrate that a heterogeneously charged surface induces an inhomogeneous potential of the uncharged membrane if separations are small enough. The theoretical predictions shown in Fig. 5 are in good qualitative agreement with the simulation results.

Our results show that at $h > L$ the membrane potential is uniform and does not vary with y , which is in agreement with earlier predictions made for impermeable surfaces.¹³ At small $h < L$ there are pronounced variations of the induced membrane potential in the y -direction, and its sign coincides with that of the charge patches of the wall. Note that for a very small $\kappa_i h \ll 1$ and a strong screening, $\kappa_i L > 1$, the distribution of the membrane potential becomes locally uniform within each stripe L_1 or L_2 . The net membrane potential is then given merely by a sum of independent contributions of each charged stripe. Such a superposition approximation has been previously used to describe heterogeneously charged impermeable walls separated by a film of an arbitrary thickness.⁵⁰ We see that in the case of a membrane the range of applicability of this model is much smaller.

Fig. 6 shows the disjoining pressure in the gap between the striped wall and the membrane at fixed $\kappa_i L = 10$. We also fix an average charge of the wall, $b_0\kappa_i^{-1} = -1$, and $\omega = 0.5$, but vary the surface heterogeneity, $b_1 - b_2$. It can be seen that for large $\kappa_i h$ (above 3 for our parameters) the heterogeneity of the wall does not play

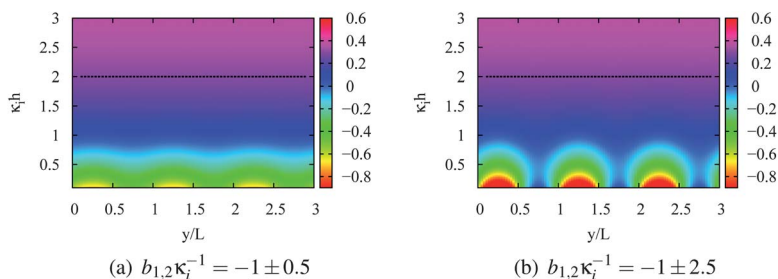


Fig. 5 Membrane potential, ϕ^m , (colorbar shows the color scale) as a function of $\kappa_i h$ and y/L calculated at $\bar{Z} = -1$, $\kappa_i L = 2$, and $b_0\kappa_i^{-1} = -1$. The dashed line shows the distance from the wall $h = L$.

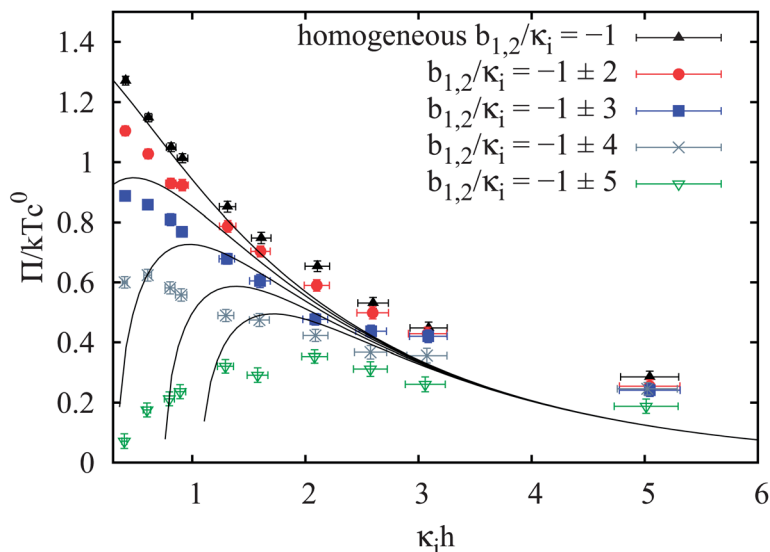


Fig. 6 Disjoining pressure in the gap between a heterogeneously charged wall and a semipermeable membrane ($\kappa_1 L = 10$). The curves show the predictions of the linearized PB theory, and the symbols show the simulation results.

any role. However, at smaller $\kappa_1 h$ there is a discrepancy from the reference homogeneous system, especially where the heterogeneity is higher. The discrepancy is always in the direction of a smaller pressure than that predicted for a homogeneously charged wall. Therefore, the contribution from the heterogeneity can be seen as an additional attractive force acting in the system. Simple arguments given below justify this conclusion. Indeed, if $\kappa_1 h \gg 1$, one can derive

$$\left(\frac{\Pi(h)}{k_B T c_0}\right)^2 \approx \left(\frac{\Pi_0(h)}{k_B T c_0}\right)^2 - \frac{(b_1 - b_2)^2 (\eta - 1)}{\kappa_i^2 \eta + 1} \omega(1 - \omega) e^{-2q_1 h} \quad (21)$$

The second (negative) term can be interpreted as an exponentially decaying (weak) attractive force with the characteristic length q_1^{-1} . For $\kappa_1 h \ll 1$, we get

$$\left(\frac{\Pi(h)}{k_B T c_0}\right)^2 \approx \left(\frac{\Pi_0(h)}{k_B T c_0}\right)^2 + \frac{(b_1 - b_2)^2 \bar{Z} \omega(1 - \omega)}{\kappa_i^2 \eta^2 2} \quad (22)$$

The second term of this expression is again negative (*i.e.* attractive), but of much larger amplitude, which allows us to interpret the results presented in Fig. 6. In particular, it explains a stronger attraction for more heterogeneous (*i.e.* with larger $b_1 - b_2$) surfaces.

5 Conclusions and perspectives

In this paper, we have considered the effect of surface charge heterogeneity on the electrostatic interaction with a neutral semipermeable membrane in contact with a bulk reservoir of an electrolyte solution. Two approaches have been followed. First, we have used continuum electrostatics, namely, a linearized PB approach, to propose a macroscopic estimate of the electrostatic disjoining pressure

associated with a surface characterized by a heterogeneous (striped) charge pattern. This (analytical) approach has enabled us to determine the important factors controlling the electrostatic interaction with a membrane. In particular, we have demonstrated that the membrane potential can be tuned by a charged wall located near the membrane, so that a membrane can take a heterogeneous electrostatic potential. We have also shown that surface heterogeneity becomes important at low net surface charge, large $\kappa_i L$ and relatively small, compared to L , distances. In this case, heterogeneity reduces the repulsive disjoining pressure as compared with that expected for a uniformly charged wall. In other situations the patterned surface can be treated as a homogeneous one. Then on the basis of Langevin dynamics simulations we have verified our theory for weakly charged surfaces and small $\kappa_i h$. However, a discrepancy between the two approaches is exhibited at large $\kappa_i h$ and/or strongly charged surfaces. This points out the importance of the nonlinear effects in the full PB theory.

In our paper, we presented results on the repulsive interaction associated with a surface formed by alternating stripes of different local charge and a neutral semi-permeable membrane in contact with a water–electrolyte solution. However, our results can be easily extended to more complex patterns, relevant to artificial and biological systems, to charged membranes, and polyelectrolyte systems. As some examples, the heterogeneity may have a dramatic implication on the cell adhesion since it is known to be controlled by non-specific forces such as long-range electrostatics.⁵¹ Additionally, similar to ref. 52 we propose that the neighbouring charged objects affect the state of the cell membrane surface and cell interactions, as well as complicated biological processes such as endocytosis and signalling processes through altering the membrane potential. Finally, the induced potential could change the conformation of the membrane proteins, which in turn could affect the ion channels. Note that such complex systems cannot be solved in an analytical way. Still, we believe that our study suggests a promising way towards understanding some basic physics underlying the behavior of these biological systems.

Acknowledgements

This work was supported by the Russian Foundation for Basic Research (grant 12-03-00916) and SFB 985 “Functional microgels and microgel systems”. Access to computational resources at the Center for Parallel Computing at the M. V. Lomonosov Moscow State University (“Lomonosov” and “Chebyshev” super-computers) is gratefully acknowledged.

References

- 1 J. N. Israelachvili, *Intermolecular and Surface Forces*, Academic Press, San Diego, 3rd edn, 2011, pp. 291–340.
- 2 K. Simons and D. Toomre, *Nat. Rev. Mol. Cell Biol.*, 2000, **1**, 31–39.
- 3 S. C. Glotzer and M. J. Solomon, *Nat. Mater.*, 2007, **6**, 557–562.
- 4 E. E. Meyer, Q. Lin, T. Hassenkam, E. Oroudjev and J. N. Israelachvili, *Proc. Natl. Acad. Sci. U. S. A.*, 2005, **102**, 6839–6842.
- 5 I. Popa, G. Papastavrou and M. Borkovec, *Phys. Chem. Chem. Phys.*, 2010, **12**, 4863–4871.
- 6 W. Chen, S. Tan, Z. Huang, T.-K. Ng, W. T. Ford and P. Tong, *Phys. Rev. E: Stat., Nonlinear, Soft Matter Phys.*, 2006, **74**, 021406.
- 7 A. Walther and A. H. E. Muller, *Soft Matter*, 2008, **4**, 663–668.
- 8 J. Du and R. K. O'Reilly, *Chem. Soc. Rev.*, 2011, **40**, 2402–2416.

- 9 A. B. Pawar and I. Kretzschmar, *Macromol. Rapid Commun.*, 2010, **31**, 150–168.
- 10 R. Vreeker, A. J. Kuin, D. C. D. Boer, L. L. Hoekstra and W. G. M. Agterof, *J. Colloid Interface Sci.*, 1992, **154**, 138–145.
- 11 S. Perkin, N. Kampf and J. Klein, *Phys. Rev. Lett.*, 2006, **96**, 038301.
- 12 V. M. Muller and B. V. Derjaguin, *Colloids Surf.*, 1983, **6**, 205–220.
- 13 S. J. Miklavic, D. Y. C. Chan, L. R. White and T. W. Healy, *J. Phys. Chem.*, 1994, **98**, 9022–9032.
- 14 S. J. Miklavcic, *J. Chem. Phys.*, 1995, **103**, 4794–4806.
- 15 D. Ben-Yaakov, D. Andelman and H. Diamant, *Phys. Rev. E: Stat., Nonlinear, Soft Matter Phys.*, 2013, **87**, 022402.
- 16 R. Brewster, P. A. Pincus and S. A. Safran, *Phys. Rev. Lett.*, 2008, **101**, 128101.
- 17 Y. S. Jho, R. Brewster, S. A. Safran and P. A. Pincus, *Langmuir*, 2011, **27**, 4439–4446.
- 18 N. Boon and R. van Roij, *J. Chem. Phys.*, 2011, **134**, 054706.
- 19 M. Lindemann and M. Winterhalter, *IEE Proc. Syst. Biol.*, 2006, **153**, 107.
- 20 E. Donath, G. B. Sukhorukov, F. Caruso, S. A. Davis and H. Möhwald, *Angew. Chem., Int. Ed.*, 1998, **37**, 2202–2205.
- 21 O. I. Vinogradova, O. V. Lebedeva and B. S. Kim, *Annu. Rev. Mater. Res.*, 2006, **36**, 143.
- 22 B. S. Kim, V. Lobaskin, R. Tsekov and O. I. Vinogradova, *J. Chem. Phys.*, 2007, **126**, 244901.
- 23 O. I. Vinogradova, D. Andrienko, V. V. Lulevich, S. Nordschild and G. B. Sukhorukov, *Macromolecules*, 2004, **37**, 1113.
- 24 T. Odijk and F. Slok, *J. Phys. Chem. B*, 2003, **107**, 8074–8077.
- 25 B. Alberts, D. Bray, J. Lewis, M. Raff, K. Roberts and J. D. Watson, *Molecular Biology of the Cell*, Garland Publishing, NY & London, 1983.
- 26 K. Sen, J. Hellman and H. Nikaido, *J. Biol. Chem.*, 1988, **263**, 1182.
- 27 J. B. Stock, B. Rauch and S. Roseman, *J. Biol. Chem.*, 1977, **252**, 7850.
- 28 S. Sukharev, M. Betanzos, C.-S. Chiang and H. R. Guy, *Nature*, 2001, **409**, 720.
- 29 Y. Zhou and G. Stell, *J. Chem. Phys.*, 1988, **89**, 7010.
- 30 M. Deserno and H. H. von Grünberg, *Phys. Rev. E: Stat. Phys., Plasmas, Fluids, Relat. Interdiscip. Top.*, 2002, **66**, 011401.
- 31 R. Tsekov and O. I. Vinogradova, *J. Chem. Phys.*, 2007, **126**, 094901.
- 32 M. R. Stukan, V. Lobaskin, C. Holm and O. I. Vinogradova, *Phys. Rev. E: Stat., Nonlinear, Soft Matter Phys.*, 2006, **73**, 021801.
- 33 R. Tsekov, M. R. Stukan and O. I. Vinogradova, *J. Chem. Phys.*, 2008, **129**, 244707.
- 34 A. Siber, A. L. Bozic and R. Podgornik, *Phys. Chem. Chem. Phys.*, 2012, **14**, 3746–3765.
- 35 B. W. Ninham and V. A. Parsegian, *J. Theor. Biol.*, 1971, **31**, 405–428.
- 36 O. I. Vinogradova, L. Bocquet, A. N. Bogdanov, R. Tsekov and V. Lobaskin, *J. Chem. Phys.*, 2012, **136**, 034902.
- 37 V. A. Lobaskin, A. N. Bogdanov and O. I. Vinogradova, *Soft Matter*, 2012, **8**, 9428–9435.
- 38 D. Andelman, in *Soft Condensed Matter Physics in Molecular and Cell Biology*, ed. W. Poon and D. Andelman, Taylor & Francis, New York, 2006, ch. 6.
- 39 H. Ohshima, *J. Colloid Interface Sci.*, 2010, **350**, 249–252.
- 40 M. Deserno and H.-H. von Grünberg, *Phys. Rev. E: Stat. Phys., Plasmas, Fluids, Relat. Interdiscip. Top.*, 2002, **66**, 011401.
- 41 D. Ben-Yaakov and D. Andelman, *Phys. A*, 2010, **389**, 2956–2961.
- 42 D. Andelman, *Handbook of Biological Physics*, North-Holland, 1995, pp. 603–642.
- 43 S. D. A. Russel, W. B. and W. R. Schowalter, “*Colloidal Dispersions*”, Cambridge Univ. Press, Cambridge, 1989.
- 44 S. Bhattacharjee and M. Elimelech, *J. Chem. Phys.*, 1997, **193**, 273–285.
- 45 J. Stankovich and S. L. Carnie, *Langmuir*, 1996, **12**, 1453–1461.
- 46 H. J. Limbach, A. Arnold, B. A. Mann and C. Holm, *Comput. Phys. Commun.*, 2006, **174**, 704–727.
- 47 J. D. Weeks, D. Chandler and H. C. Andersen, *J. Chem. Phys.*, 1971, **54**, 5237–5247.
- 48 R. W. Hockney and J. W. Eastwood, *Computer Simulation Using Particles*, Taylor & Francis, 1989.
- 49 A. Arnold, J. de Joannis and C. Holm, *J. Chem. Phys.*, 2002, **117**, 2496–2502.
- 50 A. J. Kuin, *Faraday Discuss. Chem. Soc.*, 1990, **90**, 235–244.
- 51 S. Kalasin, J. Dabkowski, K. Nsslein and M. M. Santore, *Colloids Surf., B*, 2010, **76**, 489–495.
- 52 D. Gingell, *J. Theor. Biol.*, 1967, **17**, 451–482.